Effect of Short-Term Aging on the Low Cycle Fatigue Behavior of Advanced 10% Cr Steel

Roman Mishnev[a)] and Nadezhda Dudova

Belgorod State University, Belgorod, 308015 Russia

[a)] Corresponding author: mishnev91@mail.ru

Abstract. The effect of short-term aging (100 h) at 650°C on the fatigue life and low cycle fatigue (LCF) behavior at 20 and 650°C of an advanced heat-resistant martensitic 10% Cr steel with low N and high B contents was studied. It was revealed that short-term aging did not have a negative effect on fatigue life. The LCF behavior of the aged steel followed a Basquin–Manson–Coffin and Morrow relationships. Effect of precipitated Laves phase particles during aging on the LCF resistance is discussed.

INTRODUCTION

High-chromium martensitic steels are used as creep-resistant materials capable of operating in the high-temperature boiler tracts, steam pipelines and turbines of ultra-supercritical fossil power plants at metal temperatures approaching up to 650°C [1]. A new generated 10% Cr heat-resistant martensitic steel (10% Cr–2% W–0.7% Mo–3% Co–NbV) with high B (0.008%) and low N (0.003%) contents demonstrates a unique high creep resistance [2]. The high creep strength of this type of steels is attributed to the tempered martensite lath structure (TMLS) consisting of a hierarchical sequence of structural elements with high dislocation density. The stability of TMLS is provided by the nanoscale M(C, N)-type carbonitrides distributed within the ferritic matrix and $M_{23}C_6$ carbides that are located on the all type boundaries [2].

Low cycle fatigue (LCF) which is caused by cyclic thermal stresses from start-up/shut-down regimes of steam turbines, also induces transformation of the TMLS to the subgrain structure which deteriorates the creep strength. It has been shown recently how changing the LCF test regimes affects the cyclic behavior and fatigue life of the 10% Cr steel. However, aging effect on the cyclic behavior of the steel has not been yet established. It's known that the Laves phase particles precipitate on boundaries during aging that can affect the fatigue life. On the one hand, it is well known, that long-term aging can significantly reduce the fatigue life [3]. On the other hand, the Laves phase particles, precipitated during short-term aging, are comparable in particle size with $M_{23}C_6$ carbides. Since the Laves phase particles are located on the all type boundaries, this leads to an increase in the number density of boundary particles, which can significantly strengthen the lath structure [4].

The aim of the present study was to examine the effect of short-term aging at 650°C on the fatigue life of advanced 10% Cr steel containing high B and low N contents at room and elevated temperature. The fatigue life and LCF behavior of the 10% Cr steel after aging was compared with the results obtained for the tempered steel [4].

MATERIAL AND METHODS

A 10% Cr steel with the following chemical composition (in wt %) 0.1C, 0.06Si, 0.1Mn, 10.0Cr, 0.17Ni, 0.7Mo, 0.05Nb, 0.2V, 0.003N, 0.008B, 2.0W, 3.0Co, 0.002Ti, 0.006Cu, 0.01Al and Fe-balance was examined. The standard heat treatment of the steel was consisted in normalization at 1060°C/30 min and tempering at 770°C/3 h (initial state). Then the steel was subjected to aging at 650°C in air during 100 h (aged state). LCF tests were carried out at room temperature and 650°C under fully reversed tension-compression loading conditions with different constant

Proceedings of the International Conference "Physical Mesomechanics. Materials with Multilevel Hierarchical Structure and Intelligent Manufacturing Technology"
AIP Conf. Proc. 2509, 020134-1–020134-4; https://doi.org/10.1063/5.0084754
Published by AIP Publishing. 978-0-7354-4190-3/$30.00

total strain amplitudes (ε_{ac} = const) ranging from ±0.2 to ±0.6% with the ratio of minimum strain to maximum strain $R = -1$ and frequency 0.5 Hz on cylindrical specimens with a gauge length of 18 mm and a diameter of 5 mm using an Instron 8801 testing machine. The characteristic parameters of the loops were determined for $N = 0.5N_f$ to evaluate the basic fatigue properties of the steel.

RESULTS AND DISCUSSION

Initial and Aged Structure

The TMLS of the 10% Cr steel is typical for high-chromium martensitic steels and was described in detail previously [5] (Fig. 1a). In the tempered state, an average size of prior austenite grains is 35 μm. Thin martensitic laths (width is 380 nm) contain dislocations of high density (1.7×10^{14} m^{-2}) in their interiors. Nanoscale $M_{23}C_6$-type carbides with a mean size of 70 nm are located on the all type boundaries. M(C, N)-type carbonitrides with average dimensions of 30 nm are uniformly distributed in the matrix. After short-term aging at 650°C for 100 h, the lath width and dislocation density remained almost the same. In contrast, the precipitation distribution changed due to aging. The small Laves phase (Fe_2(W, Mo)) particles with the mean size of approximately 100 nm are observed (Fig. 1b). So, precipitated Laves phase particles along with fine $M_{23}C_6$ carbides with size of 70 nm are densely distributed at the lath/grain boundaries. The number density of all boundary particles increased by more than 10% from 4.6 to 5.2 μm^{-1} due to aging.

LCF Behavior

The cyclic stress response curves at 20 and 650°C for the aged 10% Cr steel are shown in Figs. 2a, 2b. It is seen that the stress level for both initial and aged states is the same. Increasing temperature led to a decrease in the stress amplitude significantly. At room temperature, the cyclic hardening or steady-state behavior occurred at first 10–40 cycles, depending on the strain amplitude. The following deformation was accompanied with the continuous cyclic softening. At 650°C, the steady-state stage was observed only at ε_{ac} = ±0.2% up to 10th cycle, whereas at higher strain amplitudes of ±0.35 and ±0.6%, the onset of cyclic softening appeared immediately after the first cycle and took place up to failure. The higher ε_{ac} resulted in the lower number of cycles to failure at both temperatures.

Figures 2c, 2d show the typical hysteresis loops recorded during the tests with different strain amplitudes for the half-life cycle. The serrations on the stress-strain curves at 650°C can be associated with dynamic strain aging effect (Fig. 2d). At 650°C and ε_{ac} = ±0.2%, stress drops are very pronounced in contrast to that in the initial state and reach 20 MPa [3].

Table 1 shows data on the fatigue life of steel in both states. It is seen that the aged steel had an advantage as compared with the tempered steel at intermediate and high strain amplitudes. An increase in the number of cycles to failure is about 12–26% at ε_{ac} = ±0.35% and reaches 70–120% at ε_{ac} = ±0.6%, depending on the temperature. At low ε_{ac} = ±0.2%, the LCF life seems to be the same order of magnitude in both states. So, the short-term aging did not lead to a decrease in the fatigue life of the 10% Cr steel. In contrast, it had a positive effect at high strain amplitude.

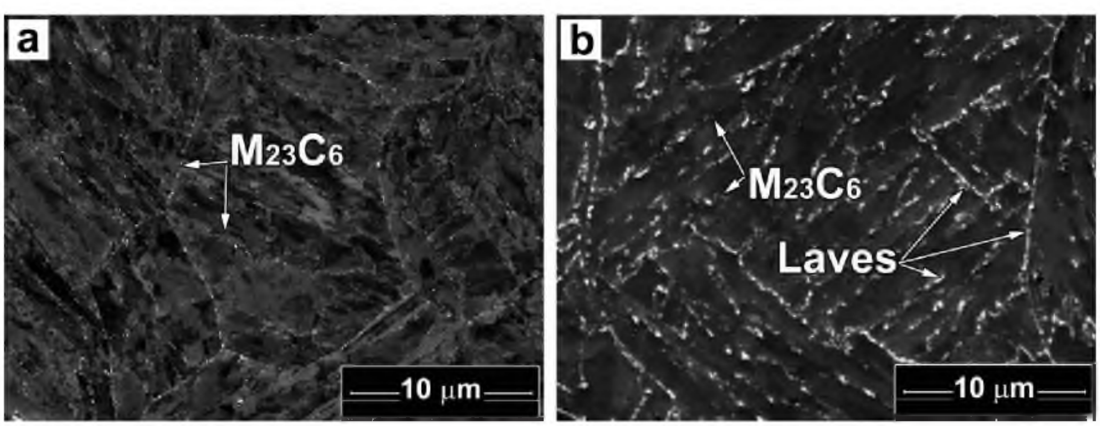

FIGURE 1. Scanning electron microscopy structure of the 10% Cr steel before (a) and after (b) aging at 650°C for 100 h.

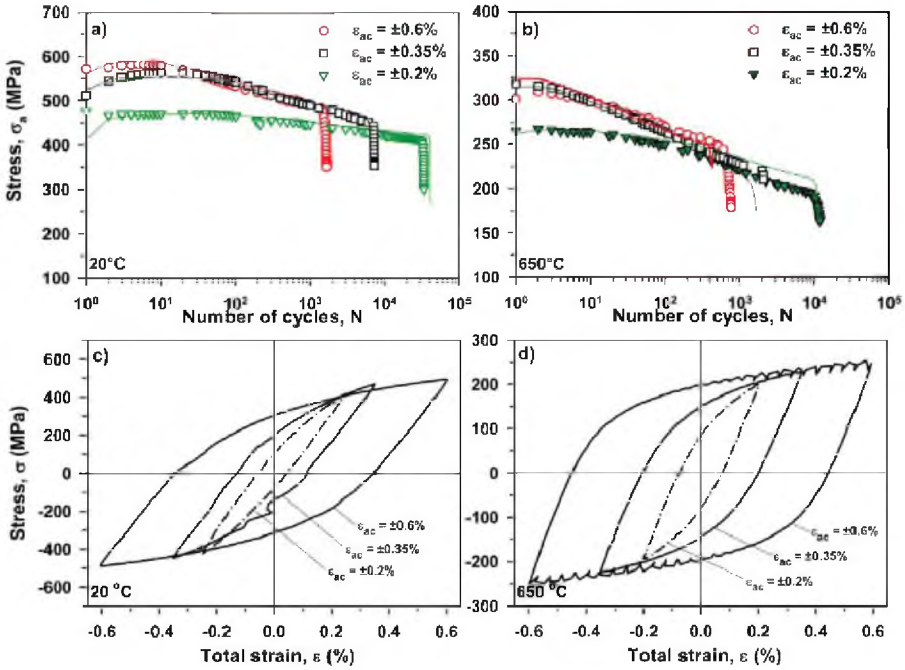

FIGURE 2. Cyclic stress response curves (a, b) of the initial (solid line) and aged (symbols) 10% Cr steel and stress–strain hysteresis loops (c, d) for the half-life cycle in aged condition.

TABLE 1. Effect of temperature and strain amplitude on the fatigue life of the initial and aged 10% Cr steel

T, °C	State	ε_{ac} = ±0.2%	ε_{ac} = ±0.35%	ε_{ac} = ±0.6%
20	Initial	41.717	6474	764
	Aged	33.776	7283	1674
650	Initial	11.137	1638	441
	Aged	11.844	2070	766

The half-life cycle stress amplitude σ_a–plastic strain amplitude ε_{ap} curves may be represented by the following power-law relationship of Morrow [6]:

$$\sigma_a = K'(\varepsilon_{ap})^{n'} \Rightarrow \lg \sigma_a = \lg K' + n' \lg \varepsilon_{ap}, \quad (1)$$

where K' is the cyclic strength coefficient and n' is the cyclic strain hardening coefficient. The corresponding relationship is shown in Fig. 3a. The values of K' and n' were determined using the method of least squares.

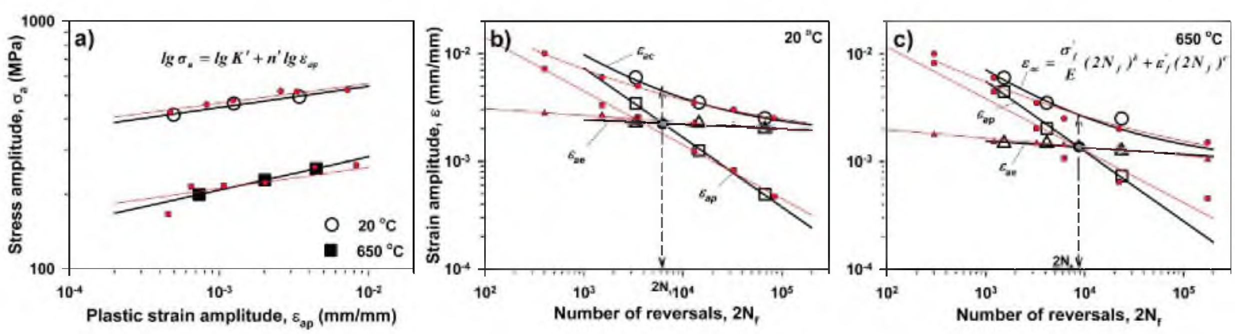

FIGURE 3. Graphical interpretation of Morrow (a) and Basquin–Manson–Coffin (b, c) equations for the initial (red dots and lines) and aged steel.

TABLE 2. Low cycle fatigue parameters of Morrow and Basquin–Manson–Coffin equations of the initial and aged 10% Cr steel

T, °C	State	K'	n'	σ'_f/E	b	ε'_f	c	$2N_t$
20	Initial	805.4	0.0796	0.00406	–0.06091	0.1416	–0.4998	3282
	Aged	809.1	0.0861	0.00328	–0.0433	0.6272	–0.6441	6270
650	Initial	511.68	0.1332	0.00287	–0.08058	0.1080	–0.4829	8285
	Aged	523.7	0.1339	0.00239	–0.0624	0.4917	–0.649	8760

The fatigue life of the aged steel as well as the tempered steel may be described by a Basquin–Manson–Coffin relationship [7–9]:

$$\varepsilon_{ac} = \varepsilon_{ae} + \varepsilon_{ap} = \sigma'_f / E(2N_f)^b + \varepsilon'_f(2N_f)^c, \quad (2)$$

where ε_{ac} is the total strain amplitude, ε_{ae} and ε_{ap} are the elastic and plastic strain amplitudes, respectively, $2N_f$ is the number of reversals to failure, σ'_f is the fatigue strength coefficient, ε'_f is the fatigue ductility coefficient, b is the fatigue strength exponent, and c is the fatigue ductility exponent. The total, elastic and plastic strain amplitudes are plotted as functions of the number of cycles to failure in Figs. 3b, 3c using a double logarithmic scale.

All parameters of Eqs. (1) and (2) for the aged steel are summarized in Table 2 in comparison with the data for the tempered steel [3]. It is seen that the K' and n' coefficients are the same for both states, which confirms that the short-term aging did not reduce the cyclic strength of the steel.

A more pronounced effect of aging is observed for the parameters of Eq. (2), which is associated with the redistribution of the contribution of plastic and elastic components to the total deformation. Moreover, the point $2N_t$, which corresponds to the intersection of two curves: ε_{ae} versus $2N_f$ and ε_{ap} versus $2N_f$, shifted to a larger number of reversals due to aging. This means that the contribution of the plastic strain to the total strain amplitude is significant up to higher reversals (6270 instead of 3282 at 20°C). This finding is in accordance with the increase in the fatigue life of steel after short-term aging. However the strain amplitude corresponding to the point $2N_t$, for the aged state is slightly lower ($\varepsilon_{ac} = 0.45\%$) than for the initial state ($\varepsilon_{ac} = 0.51\%$). In the aged state, the steel has a narrower strain range, where elastic component dominates. When tested at 650°C, aging did not change the transition strain amplitude ($\varepsilon_{ac} = 0.27\%$).

Thus, these results confirmed that the LCF behavior of the tempered and aged for 100 h steel is generally similar. It can be assumed that the steel softening due to W depletion from the ferritic matrix during aging was compensated by the strengthening due to the precipitation of small Laves phase particles at the lath/grain boundaries.

SUMMARY

It was established that the short-term aging for 100 h of the 10% Cr steel at 650°C did not have a negative effect on its low cycle fatigue life both at 20 and 650°C. In contrast, increase in the number of cycles to failure reached approximately 70–120% at $\varepsilon_{ac} = \pm 0.6\%$. Aging facilitated the dynamic strain aging phenomenon at 650°C and $\varepsilon_{ac} = \pm 0.6\%$. The Basquin–Manson–Coffin and Morrow dependencies are generally similar for both initial and aged states. It can be suggested that small Laves phase particles precipitated during short-term aging additionally with the $M_{23}C_6$ carbides stabilize the lath boundaries and impede the transformation of lath boundaries into subboundaries.

ACKNOWLEDGMENTS

The authors are grateful to the staff of the Joint Research Center, Belgorod State University, for their assistance with instrumental analysis.

REFERENCES

1. F. Abe, Engineering **1**, 211–224 (2015).
2. R. Kaibyshev, R. Mishnev, A. Fedoseeva, and N. Dudova, Mater. Sci. Forum. **879**, 36–41 (2017).
3. S. Mrozinski, G. Golanski, and A. Zielinska-Lipiec, Mater. Sci. **20**(4), 396–402 (2014).
4. R. Mishnev, N. Dudova, and R. Kaibyshev, Int. J. Fatigue **83**, 344–355 (2016).
5. R. Mishnev, N. Dudova, and R. Kaibyshev, Int. J. Fatigue **134**, 105522 (2020).
6. D. T. Raske and J. D. Morrow, in *Manual on Low Cycle Fatigue Testing* (American Society for Testing and Materials, STP 465, Philadelphia, PA, 1969), 1–26.
7. P. Verma, N. C. S. Srinivas, S. R. Singh, and V. Singh, Mater. Sci. Eng. **652**, 30–41 (2016).
8. G. Golański and S. Mroziński, Eng. Failure Analysis **35**, 692–702 (2013).
9. A. Nagesha, M. Valsan, R. Kannan, K. B. S. Rao, and S. L. Mannan, Int. J. Fatigue **24**, 1285–1293 (2002).